Oxygen Vacancies versus Fluorine at $CeO_2(111)$: A Case of Mistaken Identity?

J. Kullgren,[1] M. J. Wolf,[1,2] C. W. M. Castleton,[3] P. Mitev,[1] W. J. Briels,[4] and K. Hermansson[1,*]
[1]*Department of Chemistry–Ångström, Uppsala University, Box 538, S-751 21 Uppsala, Sweden*
[2]*Department of Physics & Astronomy, University College London, London WC1E 6BT, United Kingdom*
[3]*School of Science and Technology, Nottingham Trent University, Nottingham NG11 8NS, United Kingdom*
[4]*Computational Biophysics, Twente University, P.O. Box 217, AE Enschede 7500, The Netherlands*
(Received 26 August 2013; published 17 April 2014; publisher error corrected 21 April 2014)

We propose a resolution to the puzzle presented by the surface defects observed with STM at the (111) surface facet of CeO_2 single crystals. In the seminal paper of Esch *et al.* [Science **309**, 752 (2005)] they were identified with oxygen vacancies, but the observed behavior of these defects is inconsistent with the results of density functional theory (DFT) studies of oxygen vacancies in the literature. We resolve these inconsistencies via DFT calculations of the properties of both oxygen vacancies and fluorine impurities at $CeO_2(111)$, the latter having recently been shown to exist in high concentrations in single crystals from a widely used commercial source of such samples. We find that the simulated filled-state STM images of surface-layer oxygen vacancies and fluorine impurities are essentially identical, which would render problematic their experimental distinction by such images alone. However, we find that our theoretical results for the most stable location, mobility, and tendency to cluster, of fluorine impurities are consistent with experimental observations, in contrast to those for oxygen vacancies. Based on these results, we propose that the surface defects observed in STM experiments on CeO_2 single crystals reported heretofore were not oxygen vacancies, but fluorine impurities. Since the similarity of the simulated STM images of the two defects is due primarily to the relative energies of the $2p$ states of oxygen and fluorine ions, this confusion might also occur for other oxides which have been either doped or contaminated with fluorine.

DOI: 10.1103/PhysRevLett.112.156102 PACS numbers: 68.35.Dv, 68.37.Ef, 71.15.Mb, 82.65.+r

The reactivity of oxide surfaces is strongly affected by, and often dependent upon, the presence of defects [1,2], but the determination of the nature and properties of the predominant surface defect(s) for a particular material remains challenging. One of the most sensitive probes of surface structure, which has been applied to the study of defects at the surfaces of numerous metal oxides [3–7], is scanning tunneling microscopy (STM). The STM tunneling current depends upon both the surface topography and the local electronic structure; the latter dependence in particular implies that *ab initio* simulation can play a significant role in the interpretation of STM images. An example of this interplay between experiment and theory, and the one which is the subject of this Letter, is the ongoing attempt to understand the surface defect structure of CeO_2 (ceria), a material with broad technological applications, most notably in catalysis and fuel cell technology [8,9].

The most stable surface facet of CeO_2 is that parallel to the (111) crystallographic plane, a schematic plan view of which is shown in Fig. 1. The (111) facet has been the subject of numerous STM studies; the pioneering work was carried out on single crystals primarily at negative bias [10–12], thereby imaging the local density of occupied states derived from the $2p$ orbitals of the surface oxygen ions, as illustrated by the simulated STM image in Fig. 1. The pioneering work culminated in the study of Esch *et al.* [13], in which two types of point defect were observed; at negative bias, these appeared as dark depressions and triple protrusions, which, based upon a comparison with simulated images obtained using density functional theory (DFT), were identified with surface and subsurface oxygen vacancies, respectively. Furthermore, the concentration of depressions increased with annealing time, and they were observed to be essentially immobile at 300–400 °C, on a time scale of the order of minutes. Finally, the depressions were

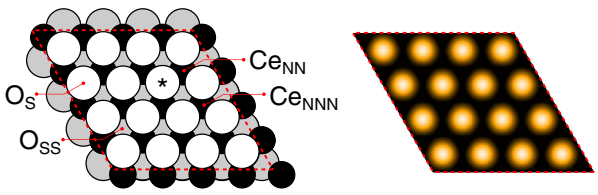

FIG. 1 (color online). Left panel: Schematic plan view of the $CeO_2(111)$ surface facet, with the $p(4\times4)$ supercell used in the simulations delineated by dashed lines. Ce, surface O and subsurface O ions are represented by black, white, and grey circles, respectively. The asterisk indicates a point defect, with respect to which the nearest-neighbor and next-nearest-neighbor cerium ions are labeled Ce_{NN} and Ce_{NNN}, respectively. Right panel: Simulated filled-state STM image of the stoichiometric surface, which highlights the sublattice formed by the surface oxygen ions.

observed to exist primarily as constituents of triangular and linear clusters after prolonged annealing.

Intriguingly, subsequent DFT calculations have predicted behavior for the oxygen vacancy which is at odds with the observations of Ref. [13] concerning the depressions, on all three of the points detailed above. More explicitly, calculations predict that the vacancy is more stable in the subsurface layer than in the surface layer [14], which would suggest that the number of surface defects should *decrease* with annealing time; that its diffusion barrier is small [15], which would render it *highly mobile* at the elevated temperatures at which the experiments were carried out; and that clustering of surface vacancies is energetically unfavourable [16], implying that they should exist primarily *in isolation*. Despite the doubt cast by these inconsistencies upon the interpretation of the defect structure of $CeO_2(111)$ in terms of oxygen vacancies alone, no alternative model has been proposed, and numerous authors have subsequently used the "vacancy model" to interpret the results of their experiments, based both on STM and on other techniques [17–20].

Recently, ceria single crystals from the same source as those used by Esch *et al.* [21], and other workers [10–12,22–29], were found to contain a concentration of fluorine of the order of 7%–10% [30], with enrichment close to the surface. Motivated by this discovery, we present herein the results of DFT calculations of the surface fluorine impurity, including its simulated filled-state STM image, which we use to compare its expected behavior with that of the oxygen vacancy. Based on these results, we propose that the "surface oxygen vacancies" observed in STM experiments on the surface of ceria single crystals were in fact fluorine impurities.

Our DFT calculations were performed under periodic boundary conditions, using the Vienna *ab initio* simulation package (VASP) [31,32]. We used the Perdew-Burke-Ernzerhof (PBE) functional [33], with a Hubbard-like U correction (DFT + U), in the form developed by Dudarev *et al.* [34], to mitigate the effects of the self-interaction error inherent to semilocal functionals such as PBE. We used an effective-U value of 5 eV, which has been shown to afford a good compromise in the accuracy of its description of both the atomic and electronic structure of ceria [35–38]. Additionally, in order to check the dependence of our simulated STM images on the choice of the functional, we generated images for the isolated defects using U values of 4 and 6 eV, and also using the hybrid functional PBE0, and found that all of these functionals produce images which are essentially indistinguishable. Further details of the calculations may be found in the Supplemental Material [39] to this Letter.

An enduring point of interest regarding the oxygen vacancy has been the localization of the two electrons left behind upon its creation via the removal of a neutral oxygen atom [14,40]. It is generally accepted that the electrons occupy f-orbitals of *individual* Ce ions, thereby breaking the symmetry of the bare vacancy, and forming (defect-bound) polarons. Our calculations of the surface oxygen vacancy agree with the most accurate theoretical simulations to date, which indicate that the electrons are well localized, and that they are most stable not on the nearest-neighbor (NN) Ce ions to the surface oxygen vacancy, as might be expected on electrostatic grounds, but on the next-nearest neighbors (NNNs), by 0.27 eV.

The fluorine atom is monovalent, and therefore a single electron is associated with its substitution into the oxygen sublattice. We find that, similarly to those associated with the oxygen vacancy, the excess electron associated with the surface fluorine is well localized on a single Ce ion. However, having calculated the total energy of the system both with the electron located on a NN Ce ion, and with it located on a NNN Ce ion, we find that, in contrast to those associated with the oxygen vacancy, the electron is most stable on a NN Ce ion, albeit by only 0.04 eV. Spin density isosurfaces associated with the localized electrons for both defects are shown in the Supplemental Material [39] to this Letter.

Simulated STM images of the surface oxygen vacancy and surface fluorine impurity, and their immediate surroundings, are shown in the left panel of Fig. 2; an experimentally obtained image from Ref. [13] is also shown for comparison. It is immediately apparent that the two simulated images are extremely similar; in particular, both defects reproduce the dark "depression" in the oxygen sublattice which is the principal feature of the experimental image. This similarity exists despite the fact that the fluorine ion *protrudes* from the surface (see the Supplemental Material [39] for further details of the defect-induced relaxation), and we must turn to the electronic structure of both defects in order to understand the origin of the similarity.

From the on-site projected densities of states (PDOSs) shown in the upper plot of the right panel of Fig. 2, one can infer that, while the dark appearance of the vacancy is due simply to the absence of the states associated with the missing surface oxygen ion, the fluorine impurity appears dark because the occupied $2p$ levels lie at a lower energy than those of the surface oxygens; due to the greater charge of the fluorine nucleus, the electrons are more tightly bound to it. That this ought to lead to an almost identical STM appearance is even clearer if one examines the difference between the PDOS of the oxygen vacancy or fluorine impurity and that of a surface oxygen ion in the stoichiometric slab, since this difference is more closely related to the contrast in an STM image. In the lower plot of the right panel of Fig. 2, one can see that it is almost identical for the two defects within the range of energies between the Fermi level and 3 eV below it; thus, for the bias voltage of −3 V used in the experiments of Esch *et al.*, the fluorine ion is as invisible as the absent oxygen associated with the vacancy.

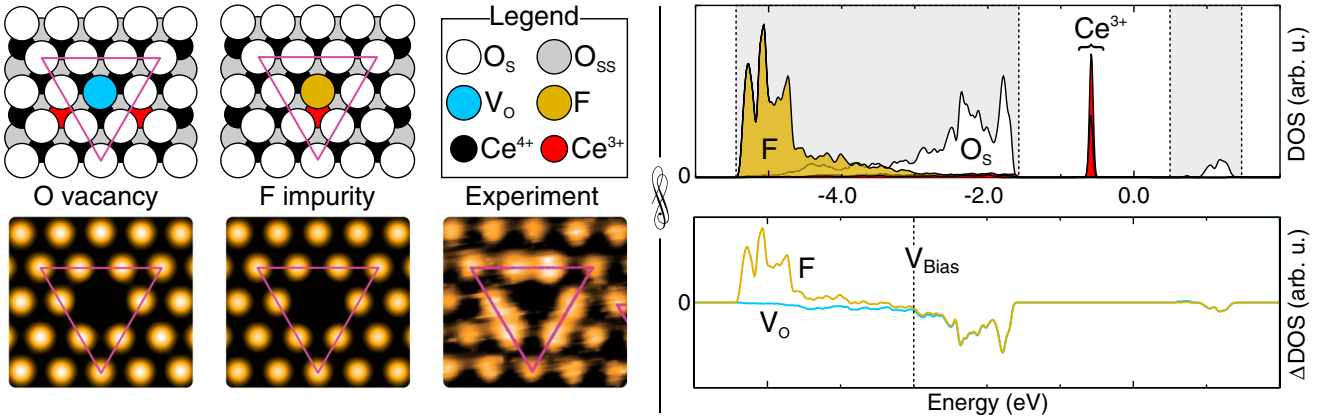

FIG. 2 (color online). Left panel: Schematic plan views (upper row) and simulated STM images (lower row) of the two defects. An experimental STM image from Ref. [13] is shown for comparison. O_S and O_{SS} stand for surface and subsurface oxygens, respectively, while V_O stands for oxygen vacancy. Right panel (Upper plot): Projected densities of states (PDOSs) of a surface oxygen (white), the surface fluorine (yellow), and the Ce^{3+} ions (red) associated with the defects. The PDOS of the surface oxygen was calculated using the stoichiometric slab, while those of the fluorine and Ce^{3+} ions were calculated using the relevant defective slabs. The PDOSs of the Ce^{3+} ions have been scaled down to one fifth of their original size, in order to improve visibility. Note that the PDOS of the two Ce^{3+} ions associated with the oxygen vacancy overlaps with that of the single Ce^{3+} ion associated with the fluorine. The band edges of the stoichiometric slab (dashed lines) are also shown. (Lower plot): Difference between the PDOS of the fluorine ion or oxygen vacancy and that of a surface oxygen ion (see text and Supplemental Material [39] for details). The energy with respect to the Fermi level, corresponding to the −3 V bias voltage used in Ref. [13], is indicated. Experimental STM image reprinted with permission from F. Esch *et al.*, Science **309**, 752 (2005). Copyright 2005, American Association for the Advancement of Science.

We note that this is due solely to the relative energies of the occupied levels on the oxygen and fluorine ions, and that as a result, it is plausible that fluorine impurities, which have been noted to be common in other oxides (see, e.g., Ref. [30] and references therein), would have a similar appearance to oxygen vacancies in filled-state STM images of their surfaces also.

Because of the similarity of the simulated STM images of the oxygen vacancy and the fluorine impurity, their experimental distinction via these images alone will likely prove difficult. We now go on to show that they may be distinguished more readily by their *stabilities relative to their subsurface counterparts*, their *mobilities*, and their *propensities to form clusters*.

We first examine the two defects' *stabilities relative to their subsurface counterparts*. In agreement with what has been found previously by other workers [14], we find that the oxygen vacancy is more stable in the subsurface layer than in the surface layer, by 0.15 eV. This would indicate that the number of surface defects should decrease in favor of subsurface defects as the sample approaches equilibrium, in contrast to the experimental observation of Esch *et al.* of a growth in the number of surface defects with prolonged annealing. However, we find that the fluorine ion is more stable in the surface layer than in the subsurface layer, by 0.48 eV, and therefore the concentration of surface fluorine would be expected to grow with increased annealing time, consistent with experimental observation.

In the experiments of Esch *et al.*, the surface defects were observed to be immobile on a time scale of the order of minutes. Thus, we now go on to examine the *mobilities* of the two defects. The height of the diffusion barrier for the surface oxygen vacancy has been calculated by other workers [15]; based on a two-step process, in which the vacancy moves between the surface and subsurface layers, the rate-limiting barrier was found to be 0.61 eV. For the fluorine ion, we consider an augmented version of this process, which proceeds via a metastable configuration in which the fluorine is on top of the surface and the vacancy is in the subsurface layer; from there, the vacancy can move back up to a neighboring surface lattice site, at which point the fluorine refills the vacancy at its new location (see Fig. 3). Using the climbing nudged-elastic-band method (CNEB) [41] with seven images (including the two end points), we find that the height of the barrier to the metastable configuration, which represents a lower bound to the barrier for the full diffusion process, is 1.47 eV (further details of the barrier calculation, including its profile, are given in the Supplemental Material [39] to this

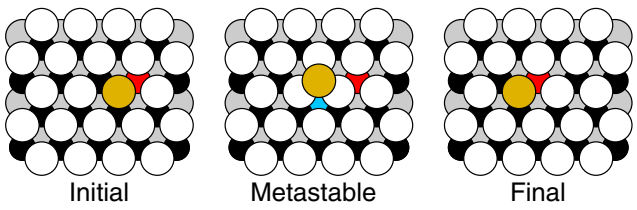

FIG. 3 (color online). Schematic plan views of the structural configurations involved in the diffusion pathway of the fluorine ion. The legend is the same as that of Fig. 2.

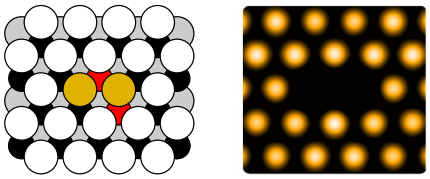

FIG. 4 (color online). Schematic plan view (left) and simulated STM image (right) of the surface fluorine pair. The legend is the same as that of Fig. 2.

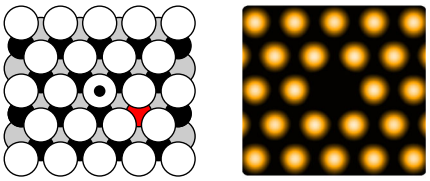

FIG. 5 (color online). Schematic plan view (left) and simulated STM image (right) of the surface hydroxyl group. The hydrogen is represented by a black dot; the legend is otherwise the same as that of Fig. 2.

Letter). In possession of the two barrier heights, we can estimate the rates of diffusion of the two defects using the Arrhenius equation: With an attempt frequency of 10^{13} Hz, which is a typical phonon frequency, and a temperature of 600 °K, which is within the temperature range used in the experiments of Esch *et al.*, we obtain a hopping frequency of 7.5×10^7 Hz using the activation energy for vacancy diffusion (0.61 eV), but 4.9 Hz using the activation energy for fluorine diffusion (1.47 eV). Clearly, the value for fluorine is in better agreement with the experiments of Esch *et al.*

Finally, we have determined whether or not oxygen vacancies or fluorine impurities exhibit a *propensity to form clusters* at the surface. In the experiments of Esch *et al.*, the surface defects were observed to exist primarily as constituents of triangular and linear clusters after prolonged annealing; in contrast, previous DFT studies [16] have found that oxygen vacancy clusters at the surface are not energetically favorable with respect to isolated vacancies. We have calculated the energy of two fluorine impurities located next to one another in the surface layer, for all six symmetrically inequivalent combinations of nearest-neighbor localized electrons; the simulated STM image of such a defect is shown in Fig. 4, along with a schematic representation showing the lowest-energy electron-localization pattern. Significantly, we find that the formation of such a pair *is* energetically favorable with respect to two isolated impurities, with a binding energy of 0.08 eV for the lowest energy configuration. A more comprehensive investigation of the formation and properties of fluorine and fluorine-vacancy clusters at the ceria (111) surface facet is currently underway, and will be the subject of a forthcoming paper.

The results of our DFT calculations show clearly that the behavior of the surface fluorine impurity is more consistent with experimental observation than the oxygen vacancy. However, our work also raises the question of what other defects could be mistaken for an oxygen vacancy at the surface. One obvious candidate is hydrogen, which was recently shown to exhibit a similar STM appearance to anion vacancies at III-V semiconductor surfaces [42]. Hydrogen is a ubiquitous contaminant, with many sources, not least the dissociation of water molecules, which are usually present even under ultrahigh vacuum conditions. To investigate this possibility, we have produced the simulated STM image of a surface hydroxyl group, which is shown in Fig. 5, and found it to be identical to those of the F impurity and the oxygen vacancy. However, we do not believe that this corresponds to the surface defect seen in the experiments of Esch *et al.*, given the high temperature at which the experiments were performed, and also given that the number of defects was observed to increase with annealing time. However, we note that such species could play a role in STM experiments conducted at lower temperatures, or in a softer vacuum.

We note that the apparent pairing of the oxygen ions neighboring the surface defect is reproduced in the simulated images of neither the oxygen vacancy nor the fluorine impurity using the $p(4 \times 4)$ supercell. We are able to reproduce the pairing only when using the $p(2 \times 2)$ cell employed by Esch *et al.*, indicating that this aspect of the agreement between theory and experiment reported by the latter authors was an artefact of their smaller supercell. We ascribe the discrepancy to tip-induced effects which are not taken into account under the Tersoff-Hamann approximation, while noting that this point does not invalidate the fact that the behavior of the fluorine impurity is in better agreement with the experimental observations of Esch than that of the oxygen vacancy.

In conclusion, we have presented the results of theoretical calculations of the fluorine impurity at the (111) surface facet of ceria, motivated by the recent report of high concentrations of fluorine in single-crystalline samples of the material, and compared its expected behavior with that of the surface oxygen vacancy, and that of the surface defects observed in the atomically-resolved STM experiments of Esch *et al.* We find that the two defects produce simulated filled-state STM images which are indistinguishable, but that their energetics and kinetics are qualitatively different; specifically, we find that the fluorine impurity is most stable in the surface layer, has a low mobility, and that it is energetically favorable for it to form clusters. These last three findings are in contrast to the vacancy, but in agreement with experimental observation; thus, our results suggest that what have been previously believed to be surface oxygen vacancies may in fact be fluorine impurities.

This work was supported by the Swedish Research Council (VR), and the European Union through the COST

Action CM1104 "Reducible Oxide Chemistry, Structure and Functions." Parts of the simulations were performed on resources provided by the Swedish National Infrastructure for Computing (SNIC) at UPPMAX and NSC, and also on the facilities of HECToR, the UK's national high-performance computing service, via the Materials Chemistry Consortium with EPSRC Grant No. EP/L000202. We would also like to acknowledge STINT (the Swedish Foundation for International Cooperation in Research and Higher Education) and the national Swedish strategic e-science program eSSENCE. Finally, we would like to thank A. L. Shluger and G. Teobaldi for useful discussions. J. Kullgren and M. J. Wolf contributed equally to this work.

*Corresponding author.
kersti@kemi.uu.se

[1] V. E. Henrich and P. Cox, *The Surface Science of Metal Oxides* (Cambridge University Press, Cambridge, England, 1996).
[2] G. Ertl and H. Knözinger, *Handbook of Heterogeneous Catalysis* (Wiley-VCH, Weinheim, 2008).
[3] U. Diebold, J. F. Anderson, K.-O. Ng, and D. Vanderbilt, Phys. Rev. Lett. **77**, 1322 (1996).
[4] O. Bikondoa, C. L. Pang, R. Ithnin, C. A. Muryn, H. Onishi, and G. Thornton, Nat. Mater. **5**, 189 (2006).
[5] U. Diebold, L. V. Koplitz, and O. Dulub, Appl. Surf. Sci. **237**, 336 (2004).
[6] M. Kulawik, N. Nilius, H.-P. Rust, and H.-J. Freund, Phys. Rev. Lett. **91**, 256101 (2003).
[7] M. Sterrer, M. Heyde, M. Novicki, N. Nilius, T. Risse, H.-P. Rust, G. Pacchioni, and H.-J. Freund, J. Phys. Chem. B **110**, 46 (2006).
[8] A. Trovarelli, *Catalysis by Ceria and Related Materials* (Imperial College Press, London, 2002).
[9] S. Park, J. M. Vohs, and R. J. Gorte, Nature (London) **404**, 265 (2000).
[10] H. Nörenberg and G. A. D. Briggs, Phys. Rev. Lett. **79**, 4222 (1997).
[11] H. Nörenberg and G. A. D. Briggs, Surf. Sci. **424**, L352 (1999).
[12] Y. Namai, K. Fukui, and Y. Iwasawa, Catal. Today **85**, 79 (2003).
[13] F. Esch, S. Fabris, L. Zhou, T. Montini, C. Africh, P. Fornasiero, G. Comelli, and R. Rosei, Science **309**, 752 (2005).
[14] M. V. Ganduglia-Pirovano, J. L. F. DaSilva, and J. Sauer, Phys. Rev. Lett. **102**, 026101 (2009).
[15] H.-Y. Li, H.-F. Wang, Y.-L. Guo, G.-Z. Lu, and P. Hu, Chem. Commun. (Cambridge) **47**, 6105 (2011).
[16] J. C. Conesa, Catal. Today **143**, 315 (2009).
[17] C. J. Weststrate, R. Westerstrom, E. Lundgren, A. Mikkelsen, J. N. Andersen, and A. Resta, J. Phys. Chem. C **113**, 724 (2009).
[18] Y. Zhou, J. M. Perket, and J. Zhou, J. Phys. Chem. C **114**, 11 853 (2010).
[19] D. C. Grinter, R. Ithnin, C. L. Pang, and G. Thornton, J. Phys. Chem. C **114**, 17 036 (2010).
[20] X. Shao, J.-F. Jerratsch, N. Nilius, and H.-J. Freund, Phys. Chem. Chem. Phys. **13**, 12 646 (2011).
[21] F. Esch (private communication).
[22] H. Nörenberg and G. A. D. Briggs, Surf. Sci. **433**, 127 (1999).
[23] K. Fukui, Y. Namai, and Y. Iwasawa, Appl. Surf. Sci. **188**, 252 (2002).
[24] Y. Namai, K. Fukui, and Y. Iwasawa, J. Phys. Chem. B **107**, 11 666 (2003).
[25] S. Gritschneder, Y. Namai, Y. Iwasawa, and M. Reichling, Nanotechnology **16**, S41 (2005).
[26] S. Torbrügge, M. Cranney, and M. Reichling, Appl. Phys. Lett. **93**, 073112 (2008).
[27] S. Torbrügge, M. Reichling, A. Ishiyama, S. Morita, and O. Custance, Phys. Rev. Lett. **99**, 056101 (2007).
[28] S. Gritschneder and M. Reichling, Nanotechnology **18**, 044024 (2007).
[29] S. Gritschneder, Y. Namai, Y. Iwasawa, and M. Reichling, Nanotechnology **16**, S41 (2005).
[30] H. H. Pieper, C. Derks, M. H. Zoellner, R. Olbrich, L. Troger, T. Schroeder, M. Neumann, and M. Reichling, Phys. Chem. Chem. Phys. **14**, 15 361 (2012).
[31] G. Kresse and J. Hafner, Phys. Rev. B **49**, 14251 (1994).
[32] G. Kresse and J. Furthmüller, Comput. Mater. Sci. **6**, 15 (1996).
[33] J. P. Perdew, K. Burke, and M. Ernzerhof, Phys. Rev. Lett. **77**, 3865 (1996).
[34] S. L. Dudarev, G. A. Botton, S. Y. Savrasov, C. J. Humphreys, and A. P. Sutton, Phys. Rev. B **57**, 1505 (1998).
[35] D. A. Andersson, S. I. Simak, B. Johansson, I. A. Abrikosov, and N. V. Skorodumova, Phys. Rev. B **75**, 035109 (2007).
[36] J. L. F. DaSilva, M. V. Ganduglia-Pirovano, J. Sauer, V. Bayer, and G. Kresse, Phys. Rev. B **75**, 045121 (2007).
[37] C. W. M. Castleton, J. Kullgren, and K. Hermansson, J. Chem. Phys. **127**, 244704 (2007).
[38] C. Loschen, J. Carrasco, K. M. Neyman, and F. Illas, Phys. Rev. B **75**, 035115 (2007).
[39] See Supplemental Material at http://link.aps.org/supplemental/10.1103/PhysRevLett.112.156102 for further details of the computational method; images depicting the relaxed atomic structures, atomic relaxation, and electronic spin densities associated with the fluorine impurity and the oxygen vacancy at the surface; and a detailed discussion of the calculation of the fluorine diffusion barrier.
[40] H.-Y. Li, H.-F. Wang, X.-Q. Gong, Y.-L. Guo, Y. Guo, G. Lu, and P. Hu, Phys. Rev. B **79**, 193401 (2009).
[41] G. Henkelman, B. P. Uberuaga, and H. Jónsson, J. Chem. Phys. **113**, 9901 (2000).
[42] C. W. M. Castleton, A. Höglund, M. Göthelid, M. C. Qian, and S. Mirbt, Phys. Rev. B **88**, 045319 (2013).